

University of Wisconsin - Madison

MADPH-02-1316

December 2002

HIGH-ENERGY NEUTRINO ASTRONOMY: SCIENCE AND FIRST RESULTS*

FRANCIS HALZEN

*Department of Physics, University of Wisconsin,
1150 University Avenue, Madison, WI 53706*

Abstract. We introduce neutrino astronomy starting from the observational fact that Nature accelerates protons and photons to energies in excess of 10^{20} and 10^{13} eV, respectively. Although the discovery of cosmic rays dates back a century, we do not know how and where they are accelerated. We review the observations as well as speculations about the sources. Among these gamma ray bursts and active galaxies represent well-motivated speculations because these are also the sources of the highest energy gamma rays, with emission observed up to 20 TeV, possibly higher.

We discuss why cosmic accelerators are expected to be cosmic beam dumps producing neutrino beams associated with the highest energy cosmic rays. Cosmic ray sources may produce neutrinos from MeV to EeV energy by a variety of mechanisms. The important conclusion is that, independently of the specific blueprint of the source, it takes a kilometer-scale neutrino observatory to detect the neutrino beam associated with the highest energy cosmic rays and gamma rays. The technology for commissioning such instrument has been established by the AMANDA detector at the South Pole. We review its performance and, with several thousand neutrinos collected, its first scientific results.

1. The Highest Energy Particles: Cosmic Rays, Photons and Neutrinos

1.1. THE NEW ASTRONOMY

While conventional astronomy spans 60 octaves in photon frequency, from 10^4 cm radio-waves to 10^{-14} cm gamma rays of GeV energy, successful efforts are underway to probe the Universe at yet smaller wavelengths and

*Talk presented at the 9th Course of Astrofundamental Physics, International School of Astrophysics D. Chalonge, Palermo, Sicily, Sept. 2002.

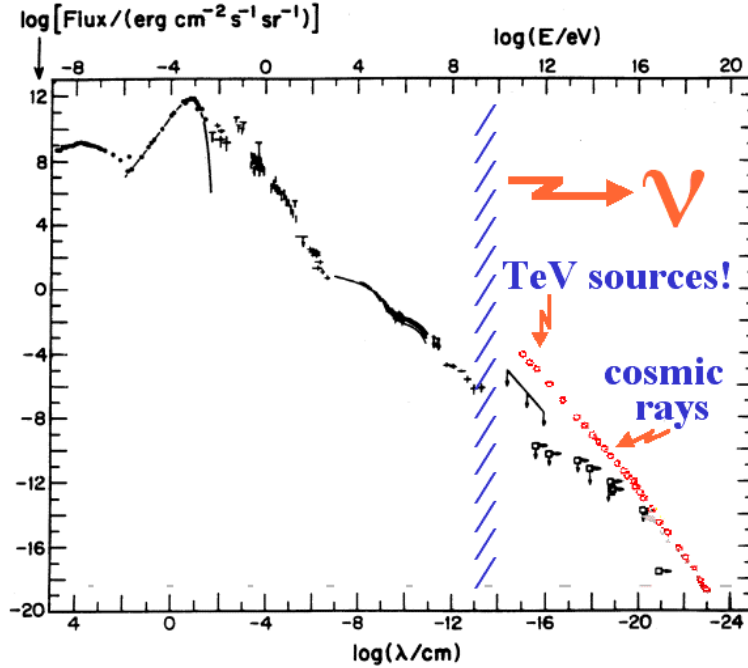


Figure 1. The diffuse flux of photons in the Universe, from radio waves to GeV-photons. Above tens of GeV, only limits are reported although individual sources emitting TeV gamma rays have been identified. Above GeV energy, cosmic rays dominate the spectrum.

larger photon energies; see Fig. 1. Gamma rays, gravitational waves, neutrinos and very high-energy protons are explored as astronomical messengers. As exemplified time and again, the development of novel ways of looking into space invariably results in the discovery of unanticipated phenomena. As is the case with new accelerators, observing the predicted is somewhat disappointing.

Why pursue high-energy astronomy with neutrinos or protons despite the considerable instrumental challenges? A mundane reason is that the Universe is not transparent to photons of TeV energy and above (in ascending factors of 10^3 , units are: GeV/TeV/PeV/EeV/ZeV). For instance, a PeV energy photon cannot deliver information from a source at the edge of our own galaxy because it will annihilate into an electron pair in an encounter with a 2.7 Kelvin microwave photon before reaching our telescope. Only neutrinos can reach us without attenuation from the edge of the Universe at all energies.

At EeV energies, proton astronomy may be possible. Above 50 EeV the arrival directions of electrically charged cosmic rays are no longer scrambled

by the ambient magnetic field of our own galaxy. They point back to their sources with an accuracy determined by their gyroradius in the intergalactic magnetic field B :

$$\frac{\theta}{0.1^\circ} \cong \frac{\left(\frac{d}{1 \text{ Mpc}}\right) \left(\frac{B}{10^{-9} \text{ G}}\right)}{\left(\frac{E}{3 \times 10^{20} \text{ eV}}\right)}, \quad (1)$$

where d is the distance to the source. Speculations on the strength of the inter-galactic magnetic field range from 10^{-7} to 10^{-12} Gauss in the local cluster. For a distance of 100 Mpc, the resolution may therefore be anywhere from sub-degree to nonexistent. Proton astronomy should be possible at the very highest energies; it may also provide indirect information on intergalactic magnetic fields. Determining their strength by conventional astronomical means has been challenging.

1.2. THE HIGHEST ENERGY COSMIC RAYS: FACTS

In October 1991, the Fly's Eye cosmic ray detector recorded an event of energy $3.0 \pm_{0.54}^{0.36} \times 10^{20}$ eV [1]. This event, together with an event recorded by the Yakutsk air shower array in May 1989 [2], of estimated energy $\sim 2 \times 10^{20}$ eV, constituted at the time the highest energies recorded. Their energy corresponds to a center of mass energy of the order of 700 TeV or ~ 50 Joules, almost 50 times the energy of the Large Hadron Collider (LHC). In fact, all active experiments [3] have detected cosmic rays in the vicinity of 100 EeV since their initial discovery by the Haverah Park air shower array [4]. The AGASA air shower array in Japan[5] has now accumulated an impressive 10 events with energy in excess of 10^{20} eV [6].

The accuracy of the energy resolution of these experiments is a critical issue. With a particle flux of order 1 event per km^2 per century, these events are studied by using the earth's atmosphere as a particle detector. The experimental signature of an extremely high-energy cosmic particle is a shower initiated by the particle. The primary particle creates an electromagnetic and hadronic cascade. The electromagnetic shower grows to a shower maximum, and is subsequently absorbed by the atmosphere. The shower can be observed by: i) sampling the electromagnetic and hadronic components when they reach the ground with an array of particle detectors such as scintillators, ii) detecting the fluorescent light emitted by atmospheric nitrogen excited by the passage of the shower particles, iii) detecting the Cerenkov light emitted by the large number of particles at shower maximum, and iv) detecting muons and neutrinos produced in the hadronic component of the air shower.

The bottom line on energy measurement is that, at this time, several experiments using the first two techniques agree on the energy of EeV-showers

within a resolution of $\sim 25\%$. Additionally, there is a systematic error of order 10% associated with the modeling of the showers. All techniques are indeed subject to the ambiguity of particle simulations that involve physics beyond the LHC. If the final outcome turns out to be an erroneous inference of the energy of the shower because of new physics associated with particle interactions at the Λ_{QCD} scale, we will have to contemplate that discovery instead.

The premier experiments, HiRes and AGASA, agree that cosmic rays with energy in excess of 10 EeV are not galactic in origin and that their spectrum extends beyond 100 EeV. They disagree on almost everything else. The AGASA experiment claims evidence that the highest energy cosmic rays come from point sources, and that they are mostly heavy nuclei. The HiRes data does not support this. Because of low statistics, interpreting the measured fluxes as a function of energy is like reading tea leaves; one cannot help however reading different messages in the spectra; see Fig. 2 and Fig. 3.

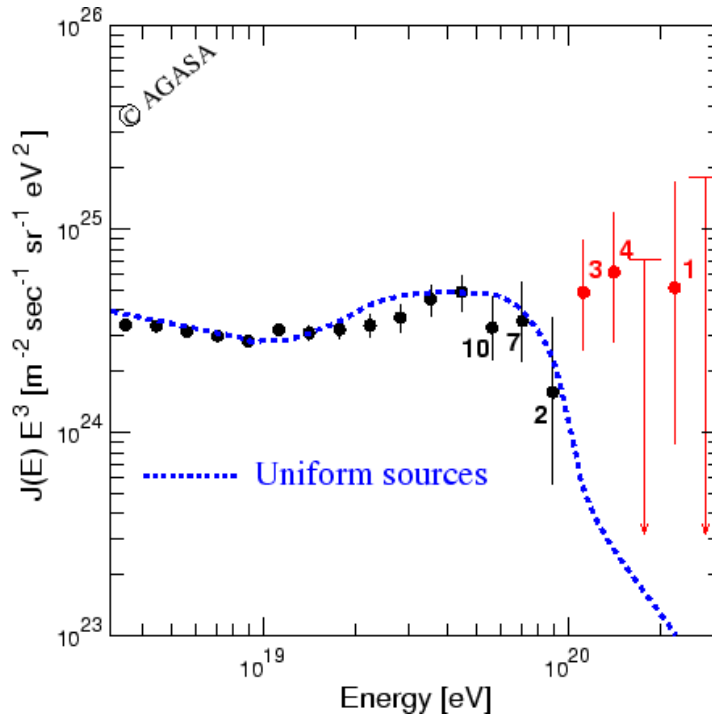


Figure 2. The cosmic ray spectrum peaks in the vicinity of 1 GeV and has features near 10^{15} and 10^{19} eV referred to as the “knee” and “ankle” in the spectrum, respectively. Shown is the flux of the highest energy cosmic rays near and beyond the ankle measured by the AGASA experiment. Note that the flux is multiplied by E^3 .

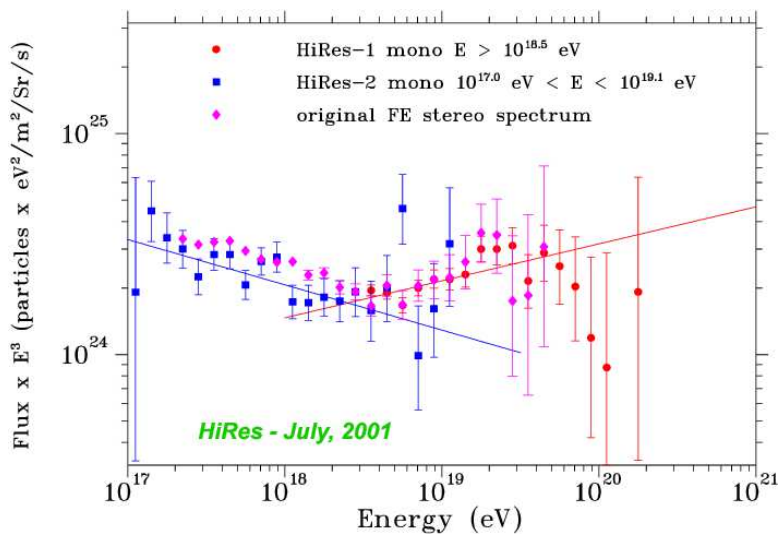


Figure 3. As in Fig. 2, results from the HiRes experiment.

1.3. THE HIGHEST ENERGY COSMIC RAYS: FANCY

1.3.1. Acceleration to $> 100 EeV$?

It is sensible to assume that, in order to accelerate a proton to energy E in a magnetic field B , the size R of the accelerator must be larger than the gyroradius of the particle:

$$R > R_{\text{gyro}} = \frac{E}{B}. \quad (2)$$

That is, the accelerating magnetic field must contain the particle orbit. This condition yields a maximum energy

$$E \sim \gamma BR \quad (3)$$

by dimensional analysis and nothing more. The γ -factor has been included to allow for the possibility that we may not be at rest in the frame of the cosmic accelerator resulting in the observation of boosted particle energies. Theorists' imagination regarding the accelerators has been limited to dense regions where exceptional gravitational forces create relativistic particle flows: the dense cores of exploding stars, inflows on supermassive black holes at the centers of active galaxies, annihilating black holes or neutron stars. All speculations involve collapsed objects and we can therefore replace R by the Schwarzschild radius

$$R \sim GM/c^2 \quad (4)$$

to obtain

$$E \propto \gamma BM. \quad (5)$$

Given the microgauss magnetic field of our galaxy, no structures are large or massive enough to reach the energies of the highest energy cosmic rays. Dimensional analysis therefore limits their sources to extragalactic objects; a few common speculations are listed in Table 1.

TABLE 1. Requirements to generate the highest energy cosmic rays in astrophysical sources.

Conditions with $E \sim 10$ EeV			
• Quasars	$\gamma \cong 1$	$B \cong 10^3$ G	$M \cong 10^9 M_{\text{sun}}$
• Blazars	$\gamma \gtrsim 10$	$B \cong 10^3$ G	$M \cong 10^9 M_{\text{sun}}$
• Neutron Stars Black Holes	$\gamma \cong 1$	$B \cong 10^{12}$ G	$M \cong M_{\text{sun}}$
• GRB	$\gamma \gtrsim 10^2$	$B \cong 10^{12}$ G	$M \cong M_{\text{sun}}$

Nearby active galactic nuclei, distant by ~ 100 Mpc and powered by a billion solar mass black holes, are candidates. With kilogauss fields, we reach 100 EeV. The jets (blazars) emitted by the central black hole could reach similar energies in accelerating substructures (blobs) boosted in our direction by Lorentz factors of 10, possibly higher. The neutron star or black hole remnant of a collapsing supermassive star could support magnetic fields of 10^{12} Gauss, possibly larger. Highly relativistic shocks with $\gamma > 10^2$ emanating from the collapsed black hole could be the origin of gamma ray bursts and, possibly, the source of the highest energy cosmic rays.

The above speculations are reinforced by the fact that the sources listed are also the sources of the highest energy gamma rays observed. At this point, however, a reality check is in order. The above dimensional analysis applies to the Fermilab accelerator: 10 kilogauss fields over several kilometers corresponds to 1 TeV. The argument holds because, with optimized design and perfect alignment of magnets, the accelerator reaches efficiencies matching the dimensional limit. It is highly questionable that nature can achieve this feat. Theorists can imagine acceleration in shocks with an efficiency of perhaps 10%.

The astrophysics of accelerating particles to Joule energies is so daunting that many believe that cosmic rays are not the beams of cosmic accelerators but the decay products of remnants from the early Universe, such as topological defects associated with a Grand Unified Theory (GUT) phase transition.

1.3.2. *Are Cosmic Rays Really Protons: the GZK Cutoff?*

All experimental signatures agree on the particle nature of the cosmic rays — they look like protons or, possibly, nuclei. We mentioned at the beginning of this article that the Universe is opaque to photons with energy in excess of tens of TeV because they annihilate into electron pairs in interactions with the infrared photon background. Protons also interact with background light, predominantly by photoproduction of the Δ -resonance, i.e. $p + \gamma_{\text{CMB}} \rightarrow \Delta \rightarrow \pi + p$ above a threshold energy E_p of about 50 EeV given by:

$$2E_p\epsilon > (m_\Delta^2 - m_p^2). \quad (6)$$

The major source of proton energy loss is photoproduction of pions on a target of cosmic microwave photons of energy ϵ . The Universe is, therefore, also opaque to the highest energy cosmic rays, with an absorption length of

$$\lambda_{\gamma p} = (n_{\text{CMB}} \sigma_{p+\gamma_{\text{CMB}}})^{-1} \cong 10 \text{ Mpc} \quad (7)$$

when their energy exceeds 50 EeV. This so-called GZK cutoff establishes a universal upper limit on the energy of the cosmic rays. The cutoff is robust, depending only on two known numbers: $n_{\text{CMB}} = 400 \text{ cm}^{-3}$ and $\sigma_{p+\gamma_{\text{CMB}}} = 10^{-28} \text{ cm}^2$.

Cosmic rays do reach us with energies exceeding 100 EeV. This presents us with three options: i) the protons are accelerated in nearby sources, ii) they do reach us from distant sources which accelerate them to even higher energies than we observe, thus exacerbating the acceleration problem, or iii) the highest energy cosmic rays are not protons.

The first possibility raises the considerable challenge of finding an appropriate accelerator in our local galactic cluster. It is not impossible that all cosmic rays are produced by the active galaxy M87, or by a nearby gamma ray burst which exploded a few hundred years ago.

Stecker [7] has speculated that the highest energy cosmic rays may be Fe nuclei with a delayed GZK cutoff. The details are complicated but the relevant quantity in the problem is $\gamma = E/AM$, where A is the atomic number and M the nucleon mass. For a fixed observed energy, the smallest boost towards GZK threshold is associated with the largest atomic mass, i.e. Fe.

1.3.3. *Could Cosmic Rays be Photons or Neutrinos?*

The above question naturally emerges in the context of models where the highest energy cosmic rays are the decay products of remnants or topological structures created in the early universe with typical energy scale of order 10^{24} eV . In these scenarios the highest energy cosmic rays are predominantly photons. A topological defect will suffer a chain decay into Grand Unified Theory (GUT) particles X and Y, that subsequently decay to familiar weak bosons, leptons and quark or gluon jets. Cosmic rays

are, therefore, predominately the fragmentation products of these jets. We know from accelerator studies that, among the fragmentation products of jets, neutral pions (decaying into photons) dominate, in number, protons by close to two orders of magnitude. Therefore, if the decay of topological defects is the source of the highest energy cosmic rays, they must be photons. This is a problem because there is compelling evidence that the highest energy cosmic rays are not photons:

1. The highest energy event observed by Fly’s Eye is not likely to be a photon [8]. A photon of 300 EeV will interact with the magnetic field of the earth far above the atmosphere and disintegrate into lower energy cascades — roughly ten at this particular energy. The detector subsequently collects light produced by the fluorescence of atmospheric nitrogen along the path of the high-energy showers traversing the atmosphere. The atmospheric shower profile of a 300 EeV photon after fragmentation in the earth’s magnetic field, is shown in Fig. 4. It disagrees with the data. The observed shower profile does fit that of a primary proton, and, possibly, that of a nucleus. The shower profile information is sufficient, however, to conclude that the event is unlikely to be of photon origin.
2. The same conclusion is reached for the Yakutsk event that is characterized by a huge number of secondary muons, inconsistent with a pure electromagnetic cascade initiated by a gamma ray.
3. The AGASA collaboration claims evidence for “point” sources above 10 EeV. The arrival directions are however smeared out in a way consistent with primaries deflected by the galactic magnetic field. Again, this indicates charged primaries and excludes photons.
4. Finally, a recent reanalysis of the Haverah Park disfavors photon origin of the primaries [4].

Neutrino primaries are definitely ruled out. Standard model neutrino physics is understood, even for EeV energy. The average x of the parton mediating the neutrino interaction is of order $x \sim \sqrt{M_W^2/s} \sim 10^{-6}$ so that the perturbative result for the neutrino-nucleus cross section is calculable from measured HERA structure functions. Because $Q^2 \sim M_W^2$, even at 100 EeV a reliable value of the cross section can be obtained based on QCD-inspired extrapolations of the structure function. The neutrino cross section is known to better than an order of magnitude. It falls 5 orders of magnitude short of the strong cross sections required to make a neutrino interact in the upper atmosphere to create an air shower.

Could EeV neutrinos be strongly interacting because of new physics? In theories with TeV-scale gravity, one can imagine that graviton exchange dominates all interactions thus erasing the difference between quarks and

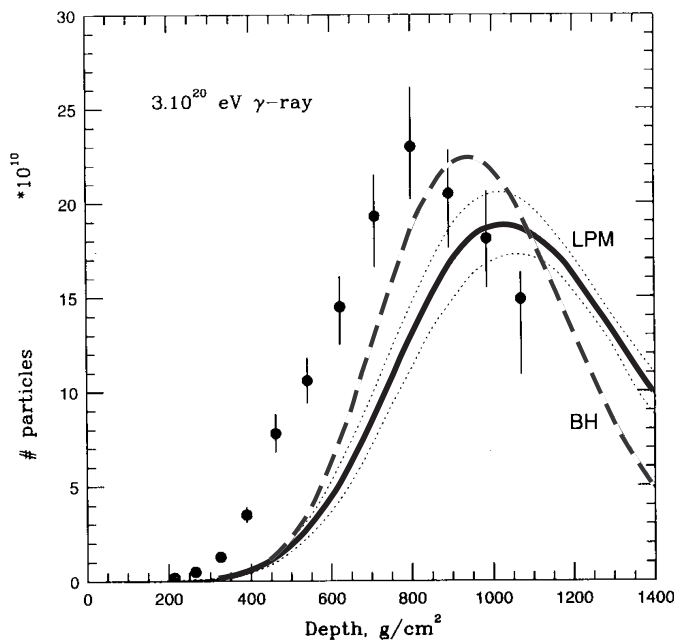


Figure 4. The composite atmospheric shower profile of a 3×10^{20} eV gamma ray shower calculated with Landau-Pomeranchuk-Migdal (dashed) and Bethe-Heitler (solid) electromagnetic cross sections. The central line shows the average shower profile and the upper and lower lines show 1σ deviations — not visible for the BH case, where lines overlap. The experimental shower profile is shown with the data points. It does not fit the profile of a photon shower.

neutrinos at the energies under consideration. The actual models performing this feat require a fast turn-on of the cross section with energy that (arguably) violates S-wave unitarity [9].

We have exhausted the possibilities. Neutrons, muons and other candidate primaries one may think of are unstable. EeV neutrons barely live long enough to reach us from sources at the edge of our galaxy.

2. A Three Prong Assault on the Cosmic Ray Puzzle

We conclude that, where the highest energy cosmic rays are concerned, both the accelerator mechanism and the particle physics are enigmatic. The mystery has inspired a worldwide effort to tackle the problem with novel experimentation including air shower arrays covering an area of several times 10^3 square kilometers[10] and arrays of multiple air Cerenkov telescopes[11]. We here discuss kilometer-scale neutrino observatories. While these have additional missions such as the search for dark matter, their observations are expected to have an impact on cosmic ray physics.

We anticipate indeed that secondary photons and neutrinos are associated with the highest energy cosmic rays; see Fig. 5. The cartoon draws our attention to the fact that cosmic accelerators are also cosmic beam dumps that produce secondary photon and neutrino beams. Accelerating particles to TeV energy and above requires relativistic, massive bulk flows. These are likely to originate from the exceptional gravitational forces associated with black holes or neutron stars. Accelerated particles therefore pass through intense radiation fields or dense clouds of gas surrounding the black hole leading to the production of secondary pions. These subsequently decay into photons and neutrinos that accompany the primary cosmic ray beam. Examples of targets for muon production include the external photon clouds and the UV radiation field that surrounds the central black hole of active galaxies, or the matter falling into the collapsed core of a dying supermassive star producing a gamma ray burst. The target material, whether a gas of particles or of photons, is likely to be sufficiently tenuous for the primary proton beam and the secondary photon beam to be only partially attenuated. However, shrouded sources from which only neutrinos can emerge, as is the case for terrestrial beam dumps at CERN and Fermilab, are also a possibility.

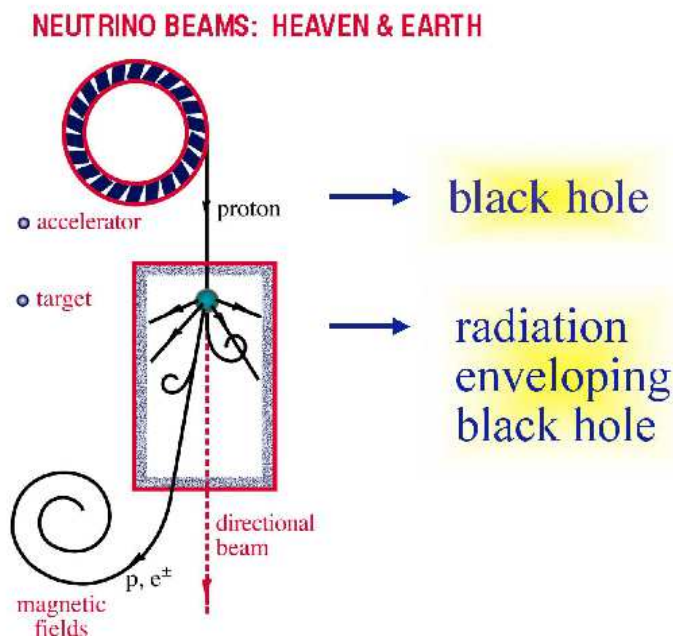


Figure 5. Diagram of cosmic accelerator and beam dump. See text for discussion.

How many neutrinos are produced in association with the cosmic ray beam? The answer to this question, among many other[12], provides the rationale for building kilometer-scale neutrino detectors.

Let's first consider the question for the accelerator beam producing neutrino beams at an accelerator laboratory. Here the target absorbs all parent protons as well as the muons, electrons and gamma rays (from $\pi^0 \rightarrow \gamma + \gamma$) produced. A pure neutrino beam exits the dump. If nature constructed such a "hidden source" in the heavens, conventional astronomy has not revealed it. It cannot be the source of the cosmic rays, however, for which the dump must be partially transparent to protons.

At the other extreme, the accelerated proton interacts, e.g. with photons in the radiation field surrounding the black hole, via the reaction

$$p + \gamma \rightarrow n + \pi^+ \text{ or } p + \pi^0. \quad (8)$$

The n, p in the final state become the observed cosmic rays and, if all particles escape without further interaction, the flux of pions and their neutrino decay products is directly related to the observed flux of cosmic rays by Eq. (8). The neutrino flux for such a transparent cosmic ray source is referred to as the Waxman-Bahcall flux [13, 14] and is shown as the horizontal lines labeled "W&B" in Fig. 6. The calculation is valid for $E \simeq 100$ PeV. When evaluating the flux at both lower and higher cosmic ray energies, larger neutrino fluxes are inferred[15, 16]. This is shown as the non-horizontal line labeled "transparent" in Fig. 6. On the lower side, the neutrino flux is higher because it is normalized to a larger cosmic ray flux. On the higher side, there are more cosmic rays in the dump to produce neutrinos because the observed flux at Earth has been reduced by absorption on microwave photons, the GZK-effect. The increased values of the neutrino flux are also shown in Fig. 6. The gamma ray flux of π^0 origin associated with a transparent source is qualitatively at the level of the observed flux of non-thermal TeV gamma rays from individual sources[17].

Nothing prevents us, however, from imagining heavenly beam dumps with target densities somewhere between those of hidden and transparent sources. When increasing the target photon density, the proton beam is absorbed in the dump and the number of neutrino-producing protons is enhanced relative to those escaping the source as cosmic rays. For the extreme source of this type, the observed cosmic rays are all decay products of neutrons with larger mean-free paths in the dump. The flux for such a source is shown as the upper horizontal line in Fig. 6.

The above fluxes are derived from the requirement that theorized neutrino sources do not overproduce cosmic rays. Similarly, observed gamma ray fluxes constrain potential neutrino sources because for every parent charged pion ($\pi^\pm \rightarrow l^\pm + \nu$), a neutral pion and two gamma rays ($\pi^0 \rightarrow$

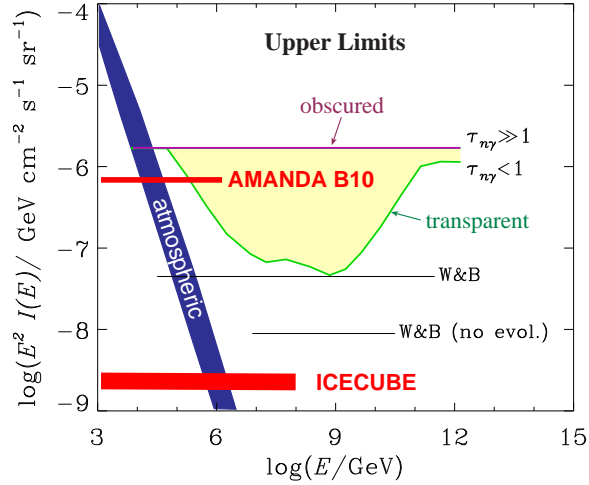


Figure 6. The neutrino flux from compact astrophysical accelerators. Shown is the range of possible neutrino fluxes associated with the the highest energy cosmic rays. The lower line, labeled “transparent”, represents a source where each cosmic ray interacts only once before escaping the object. The upper line, labeled “obscured”, represents an ideal neutrino source where all cosmic rays escape in the form of neutrons. Also shown is the ability of AMANDA and IceCube to test these models.

$\gamma + \gamma$) are produced. The electromagnetic energy associated with the decay of neutral pions should not exceed observed astronomical fluxes. These calculations must take into account cascading of the electromagnetic flux in the source and in the interstellar background photon and magnetic fields. A simple argument relating high-energy photons and neutrinos produced by secondary pions can still be derived by relating their total energy and allowing for a steeper photon flux as a result of cascading. Identifying the photon fluxes with those of non-thermal TeV photons emitted by supernova remnants and blazars, we predict neutrino fluxes at the level as the Waxman-Bahcall flux[18]. It is important to realize however that there is no evidence that TeV photons are the decay products of π^0 's. The sources of the cosmic rays have not been revealed by photon or proton astronomy [19, 20, 21, 22]; see however reference [23].

For neutrino detectors to succeed they must be sensitive to the range of fluxes covered in Fig. 6. The AMANDA detector has already entered the region of sensitivity and is eliminating specific models which predict the largest neutrino fluxes within the range of values allowed by general arguments. The IceCube detector, now under construction, is sensitive to the full range of beam dump models. IceCube will reveal the sources of the cosmic rays or derive an upper limit that will qualitatively raise the bar for solving the cosmic ray puzzle. The situation could be nothing but desperate with

the escape to top-down models being cut off by the accumulating evidence that the highest energy cosmic rays are not photons. In top-down models, decay products eventually materialize as quarks and gluons that fragment into jets of (mostly) neutrinos, few photons and very few protons[24].

3. High Energy Neutrino Telescopes

Although neutrino telescopes have multiple interdisciplinary science missions, the search for the sources of the highest-energy cosmic rays stands out because it clearly identifies the size of the detector required to do the science[25].

Whereas it has been realized for many decades that the science is compelling[26, 27, 28, 29], the real challenge has been to develop a reliable, expandable and affordable detector technology. Suggestions to use a large volume of deep ocean water for high-energy neutrino astronomy were made as early as 1960. In the case of the muon neutrino, for instance, the neutrino (ν_μ) interacts with a hydrogen or oxygen nucleus in the water and produces a muon travelling in nearly the same direction as the neutrino. The blue Cerenkov light emitted along the muon's \sim kilometer-long trajectory is detected by strings of photomultiplier tubes deployed deep below the surface. Collecting muons of neutrino origin far outside the detector, the effective detector volume exceeds the volume instrumented. With the first observation of neutrinos in the Lake Baikal and the (under-ice) South Pole neutrino telescopes, there is optimism that the technological challenges to build kilometer-scale neutrino telescopes can finally be met.

The first generation of neutrino telescopes, launched in 1975 by the bold decision of the DUMAND collaboration to construct such an instrument, are designed to reach a large telescope area and detection volume for a neutrino threshold of order 10 GeV. The optical requirements of the detector medium are severe. A large absorption length is required because it determines the spacings of the optical sensors and, to a significant extent, the cost of the detector. A long scattering length is needed to preserve the geometry of the Cerenkov pattern. Nature has been kind and offered ice and water as adequate natural Cerenkov media. Their optical properties are, in fact, complementary. Water and ice have similar attenuation length, with the role of scattering and absorption reversed. Optics seems, at present, to drive the evolution of ice and water detectors in predictable directions: towards very large telescope area in ice exploiting the long absorption length, and towards lower threshold and good muon track reconstruction in water exploiting the long scattering length.

DUMAND, the pioneering project located off the coast of Hawaii, demonstrated that muons could be detected by this technique[30], but the planned

detector was never realized. A detector composed of 96 photomultiplier tubes located deep in Lake Baikal was the first to demonstrate the detection of neutrino-induced muons in natural water[31, 32]. In the following years, *NT-200* will be operated as a neutrino telescope with an effective area between 10^3 – 5×10^3 m², depending on energy. Presumably too small to detect neutrinos from extraterrestrial sources, *NT-200* will serve as the prototype for a larger telescope. For instance, with 2000 OM, a threshold of 10–20 GeV and an effective area of 5×10^4 – 10^5 m², an expanded Baikal telescope would fill the gap between present detectors and planned larger detectors of cubic kilometer size. Its key advantage would be low threshold.

The Baikal experiment represents a proof of concept for deep ocean projects. These do however have the advantage of larger depth and optically superior water. Their challenge is to find reliable and affordable solutions to a variety of technological challenges for deploying a deep underwater detector. The European collaborations ANTARES[33, 34, 35] and NESTOR[36, 37] have planned initial deployments of large-area detectors in the Mediterranean Sea within the next year. The NEMO Collaboration is conducting site studies and R&D for a future kilometer-scale detector in the Mediterranean[38].

It is however the AMANDA detector using natural Antarctic ice that has reached the $\sim 10^4$ m² telescope area envisaged by the DUMAND project a quarter of a century ago. It has operated for 3 years with 302 optical sensors and for another 3 years with 677. More than 3000 neutrinos, well separated from background, have been collected. We concentrate on the performance and first science of this detector in the rest of the lectures.

4. The AMANDA Detector

Since 1996 the AMANDA telescope has been taking data over Antarctic winters while construction proceeds in the summer; with 80 optical modules (OM) in 1996, with 302 during 1997-1999 (AMANDA-B) and 667 OM from 2000-present (AMANDA-II). The detectors instrument 6,000 and 16,000 kilotons of ultra-transparent ice, respectively. More than 3,000 clearly identified neutrinos have been collected thus far.

The AMANDA-B high energy neutrino telescope consists of 302 optical modules on 10 strings. Each OM comprises a photomultiplier tube (PMT) with passive electronics housed in a glass pressure vessel. The OM are deployed within a cylindrical volume 120 m in diameter and 500 m in height at depths of 1500 to 2000 m below the surface of the South Pole ice cap. At this depth the optical properties of the ice are well suited for reconstructing the Cerenkov light pattern emitted by relativistic charged particles [39]. An electrical cable provides high voltage to the PMT and transmits its signals

to the surface data acquisition electronics. A light diffuser ball connected via fiber optic cable to a laser at the surface is used for calibration purposes. Copious down-going cosmic ray muons, roughly 100 every second, are also used for calibration purposes.

In January 2000, AMANDA-B was enlarged to a total of 19 strings with 667 OM to form AMANDA-II. The final detector is 200 m in diameter with approximately the same height and depth as AMANDA-B. Figure 7 shows a schematic diagram of AMANDA.

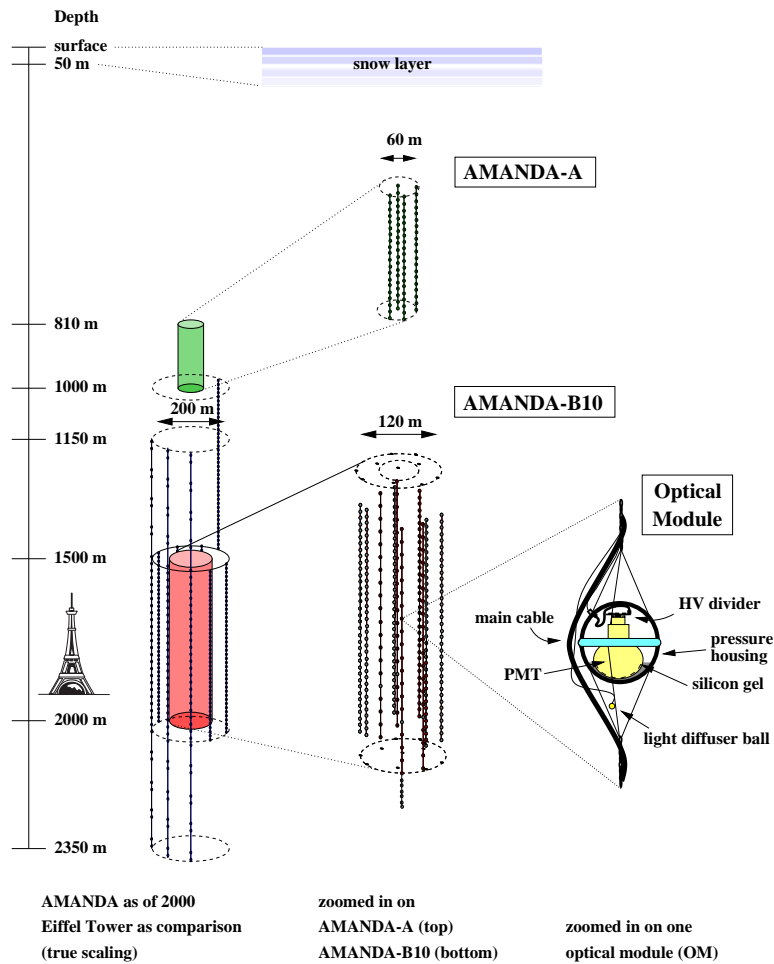


Figure 7. AMANDA-B consists of 302 optical modules in a cylindrical volume with a diameter of 120 m diameter and a height of 500 m. With an additional 9 strings, AMANDA-II (on the left) consists of 667 OM in a cylindrical volume 200 m in diameter. Both detector configurations have taken data over 3 Antarctic winters.

4.1. ATMOSPHERIC NEUTRINOS AND AMANDA CALIBRATION

AMANDA has been commissioned as a neutrino telescope in the 10,000 m² class by demonstrating its ability to reconstruct upward-going muons produced by atmospheric muon neutrinos [40, 41]. A fraction of the atmospheric muon neutrinos produced in the northern hemisphere travel through the earth, interact with the earth or the ice near AMANDA and produce muons that can be detected and reconstructed. Using data collected by AMANDA-B in 1997, they have reconstructed roughly 300 upward-going muons which are, as shown in Fig. 8, in agreement with the predicted rate and zenith angle distribution of atmospheric neutrinos produced in the northern hemisphere. The prediction is based on the extrapolation of fluxes measured at lower energies in other underground detectors and include neutrino oscillation.

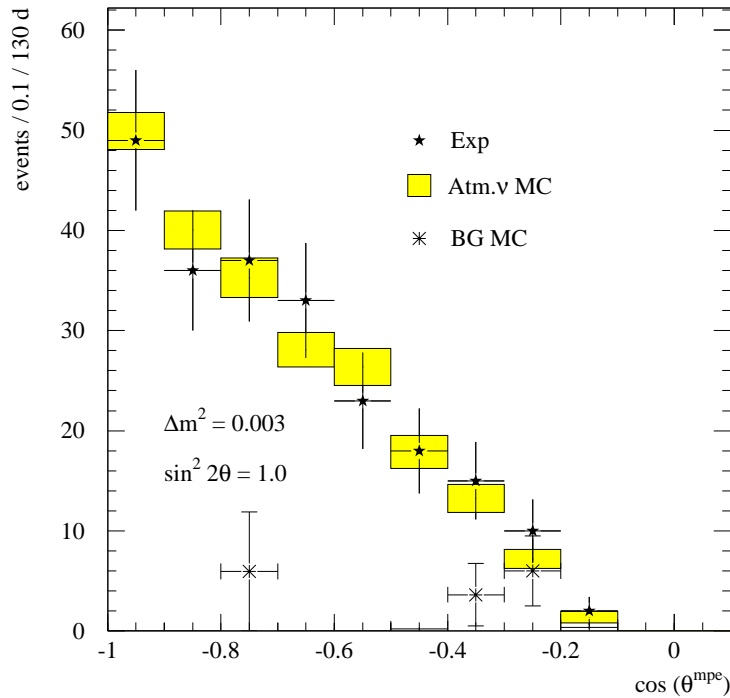


Figure 8. Number of upward-going muon events in AMANDA-B data from the Antarctic winter 1997, as a function of zenith angle ($\cos \theta = -1.0$ is vertically up in the detector). The data are shown as dots and the Monte Carlo simulation as boxes. The simulation was performed with the neutrino oscillation parameters as indicated. The predicted signal efficiency is 4% and the background level 10%, with both numbers improving near the vertical and degrading near the horizon reflecting the shape of the partially deployed detector. Simulations indicate that 90% of these events lie in an energy range $66 \text{ GeV} < E_\nu < 3.4 \text{ TeV}$.

AMANDA-B data has also been used to set competitive limits on WIMPs [42], monopoles [43] reaching one order of magnitude below the Parker bound, extremely energetic neutrinos [44], UHE ν_μ point sources [45] and diffuse fluxes [46]. The detector is also sensitive to bursts of low energy neutrinos from supernovae [47].

A preliminary analysis of atmospheric neutrino data taken with AMANDA-II in 2000 demonstrates the substantially increased effective volume of the enlarged detector. Compared to the analysis using AMANDA-B data, fewer selection criteria are required to extract a larger and qualitatively cleaner sample of atmospheric neutrino-induced muons. Because of the simplified and robust analysis, neutrino separation from background is now possible in real time and has been implemented in 2002. Figure 9 shows the excellent agreement between data and simulation achieved with a preliminary set of selection criteria applied. Note the improved angular response close to the horizon. With more sophisticated selection criteria one expects to extract at least 3 times more neutrino events in AMANDA-II relative to AMANDA-B for equivalent live-times.

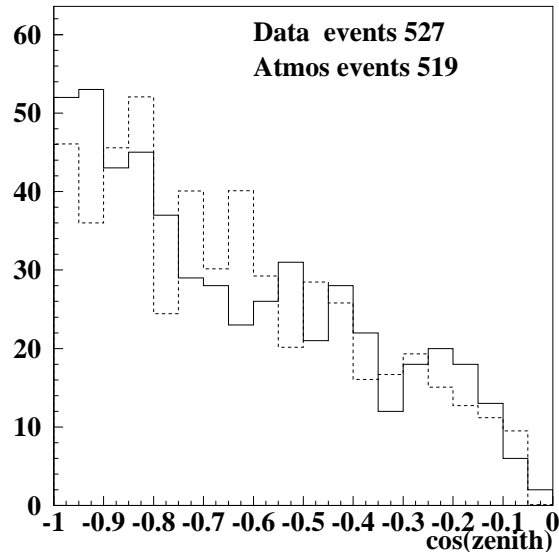


Figure 9. Number of upward-going muon events in AMANDA-II data from the year 2000 as a function of zenith angle, using a preliminary set of selection criteria. There are a total of 527 events in the data or roughly 4 per day (solid line), while 519 events are predicted by the atmospheric neutrino Monte Carlo (dashed line). Simulations indicate that these events have an energy of $100 \text{ GeV} < E_\nu < 1 \text{ TeV}$. With more sophisticated selection criteria one expects larger event rates and improved response near the horizon.

4.2. SEARCH FOR CASCADES WITH AMANDA-B AND -II

1997 AMANDA data has also been used to perform a search for the Cerenkov light produced by electromagnetic or hadronic showers (*cascades*) induced by high-energy extraterrestrial neutrinos. Demonstrating cascade sensitivity is an important step for neutrino astronomy because cascades probe all neutrino flavors, whereas the muon channel is sensitive to ν_μ only. Electron neutrinos produce cascades via the charged current interaction and all neutrino flavors produce cascades via the neutral current interaction. Cascade-like events are also produced in charged current ν_τ interactions. Compared to muons, cascades provide more accurate energy measurement, superior separation from background, but worse angular resolution. Cascades have a superior energy resolution because all energy is deposited in a small volume of ice of order 10 m diameter and because the number of Cerenkov photons scales linearly with the deposited energy. As with muons, cascades are easier to identify and reconstruct as the instrumented detector volume increases. After application of simple selection criteria that reduce the down-going muon background while preserving potential signal events, vertex position, energy and direction of the cascade are reconstructed using maximum likelihood methods. These take into account the expected Cerenkov pattern after absorption and scattering of the light in the ice [48, 49].

In the absence of a tagged source of high energy neutrino-induced cascades, one determines the response of the detector using *in-situ* light sources. The successful reconstruction of data taken with a pulsed laser and the reconstruction of isolated showers produced by the catastrophic energy loss of muons, have demonstrated that the detector is sensitive to high energy cascades [49].

The 90% C.L. limit on a diffuse flux of $\nu_e + \nu_\mu + \nu_\tau + \bar{\nu}_e + \bar{\nu}_\mu + \bar{\nu}_\tau$ for neutrino energies between 5 TeV and 300 TeV is:

$$E^2 \frac{d\Phi}{dE} < 9.8 \times 10^{-6} \text{ GeV cm}^{-2} \text{ s}^{-1} \text{ sr}^{-1}, \quad (9)$$

assuming an oscillated neutrino flux with 1:1:1 flavor composition. The 90% C.L. limit on the diffuse flux of $\nu_e + \bar{\nu}_e$ for neutrino energies between 5 TeV and 300 TeV is:

$$E^2 \frac{d\Phi}{dE} < 6.5 \times 10^{-6} \text{ GeV cm}^{-2} \text{ s}^{-1} \text{ sr}^{-1}. \quad (10)$$

Note that since the limit in Eq. (9) is on the sum of the fluxes of all neutrino flavors and the limit in Eq. (10) is on an individual flavor, the former should be divided by three when compared to the latter.

Data from AMANDA-II is currently under study and, as with the analysis of atmospheric neutrinos, preliminary results demonstrate the enhanced

power of the larger AMANDA-II detector. Angular acceptance improves to nearly 4π , backgrounds are much easier to reject, and energy acceptance improves by a factor of three to $E_\nu \sim 1$ PeV. In accordance with blind analysis procedures, 20% of the AMANDA-II data from the year 2000 has been analyzed resulting in a preliminary limit that is already lower than the one above by a factor of 3. For a source with a UHE neutrino flux at the current best limit [46], they expect eight UHE-neutrino-induced cascade events in the full 2000 dataset on an expected background of less than one event.

4.3. SEARCH FOR UHE ν_μ FROM POINT SOURCES

The AMANDA collaboration has performed a general search for the continuous emission of muon neutrinos from a spatially localized direction in the northern sky. Backgrounds are reduced by requiring a statistically significant enhancement in the number of reconstructed upward-going muons in a small bin in solid angle. The background for a particular bin can be calculated from the data by averaging over the data outside the bin in the same declination band. In contrast to the searches previously discussed, this search is more tolerant of the presence of background and the signal is therefore optimized on S/\sqrt{B} , where S represents the signal and B the background, rather than on S/B , which emphasizes signal purity.

The analysis of AMANDA-B data taken in 1997 has been reported in [45]. With AMANDA-II, one achieves larger effective area and improved sensitivity to events near the horizon because the detector has double the number of PMT and a larger lever arm in the horizontal dimension. Assuming a customary E^{-2} source spectrum, and a flux of 10^{-8} GeV cm $^{-2}$ s $^{-1}$ sr $^{-1}$, one predicts two signal and one background event in a $6^\circ \times 6^\circ$ angular bin. This flux represents an interesting benchmark because, at this level, AMANDA should observe TeV sources provided the number of gamma rays and neutrinos are roughly equal as expected from cosmic ray accelerators producing pions. Preliminary sensitivities to a sample of point sources are given in Table 2. In order to achieve blindness in this analysis the right ascension of each event (i.e., its azimuthal angle) has been scrambled. At the South Pole this effectively scrambles the event time. The data will only be unscrambled after final selection criteria have been set.

4.4. SEARCH FOR A DIFFUSE FLUX OF ν_μ NEUTRINOS

The search for diffuse sources of high energy ν_μ -induced muons is closely associated with the analysis isolating atmospheric ν_μ -induced muons as both analyses require a sample of muon tracks well separated from misreconstructed downward-going atmospheric muons. Since high-energy muons

TABLE 2. Example of AMANDA-II sensitivity to point sources in data taken in 2000. The sensitivity is defined as the predicted average limit from an ensemble of experiments with no signal, and is calculated using background levels predicted from off-source data.

Source	Declination	μ ($\times 10^{-15} \text{ cm}^{-2} \text{ s}^{-1}$)	ν ($\times 10^{-8} \text{ cm}^{-2} \text{ s}^{-1}$)
SS433	5.0	11.0	2.4
Crab	22.0	4.0	1.3
Markarian 501	39.8	2.5	1.0
Cygnus X-3	41.5	2.6	1.1
Cass. A	58.8	2.1	1.0

deposit more energy in the detector volume than low-energy muons, one isolates high energy events by requiring a high channel density, $\rho_{\text{ch}} > 3$, where the channel density is defined as the number of hit channels per 10 m tracklength. The background in the signal region is estimated by extrapolation of lower-energy data satisfying $\rho_{\text{ch}} < 3$.

Using a 20% sample of the year 2000 AMANDA-II data, 6 events satisfying all selection criteria have been identified. Simulations for a E^{-2} power law spectrum predict 3.0 events from a UHE neutrino flux at the current best limit [46] and 1.9 events from atmospheric neutrino interactions. Again a subsample of the data is used in order to achieve blindness in this analysis. The predicted average limit from an ensemble of experiments with no signal, or *sensitivity*, is roughly $1.3 \times 10^{-6} \text{ GeV cm}^{-2} \text{ s}^{-1} \text{ sr}^{-1}$, and the preliminary limit is less than roughly $10^{-6} \text{ GeV cm}^{-2} \text{ s}^{-1} \text{ sr}^{-1}$. With only 20% of the year 2000 data, AMANDA-II matches the limit obtained with the *full* sample of AMANDA-B data from 1997.

4.5. SEARCH FOR ν_{μ} FROM GRB

The search for ν_{μ} -induced muons from gamma-ray bursts (GRB) leverages temporal and directional information from satellite observations to realize a nearly background-free analysis. The steady 100 Hz cosmic ray muon background is indeed limited during the short lifetime and in the direction of a specific GRB. Assuming the broken power-law spectrum predicted by the standard fireball model[50], AMANDA has searched for muon neutrinos in coincidence with GRB. Off-source and off-time data are used to estimate background and to achieve blindness in the analysis. Data spanning the years 1997–2000 have been analyzed with roughly 500 GRB in coincidence with satellite experiments.

Detector stability over 10 s periods, a typical signal window, is an im-

portant measure of how effective this analysis can be. They have shown that the counting rate per 10 s bin in a time window of ± 1 hour around a GRB is Gaussian, revealing no instrumental effects that can mimic GRB. A limit has been obtained that reaches to within an order of magnitude of the typical event rate of 20 per kilometer square per year anticipated by fireball phenomenology[51]. With two more years of data on tape, discovery is possible, especially because the signal is mostly generated by favorable fluctuations in distance and energy of individual GRB[50].

Overall, AMANDA represents a proof of concept for the construction of a kilometer-scale neutrino observatory, IceCube.

5. IceCube: a Kilometer-Scale Neutrino Observatory

IceCube is an instrument optimized to detect and characterize neutrinos of all flavors from sub-TeV to the highest energies; see Fig. 10. It will consist of 80 kilometer-length strings, each instrumented with 60 10-inch photomultipliers spaced by 17 m. The deepest module is 2.4 km below the surface. The strings are arranged at the apexes of equilateral triangles 125 m on a side. The instrumented (not effective!) detector volume is a cubic kilometer. A surface air shower detector, IceTop, consisting of 160 Auger-style Cerenkov detectors deployed over 1 km² above IceCube, augments the deep ice component by providing a tool for calibration, background rejection and air shower physics.

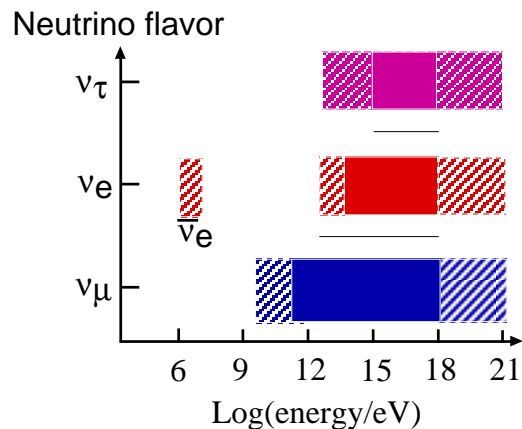


Figure 10. Although IceCube detects neutrinos of all energies and flavor above a threshold of ~ 0.1 TeV, it can identify their flavor and measure their energy only in the ranges shown.

IceCube will offer great advantages over AMANDA-II beyond its larger size: it will have a higher efficiency and superior angular resolution in re-

constructing tracks, map showers from electron- and tau-neutrinos (events where both the production and decay of a τ produced by a ν_τ can be identified) and, most importantly, measure neutrino energy. Simulations, backed by AMANDA data, indicate that the direction of muons can be determined with sub-degree accuracy and their energy measured to better than 30% in the logarithm of the energy. The direction of showers will be reconstructed to better than 10° above 10 TeV and the response in energy is linear and better than 20%. Energy resolution is critical because, once one establishes that the energy exceeds 1 PeV, there is no atmospheric muon or neutrino background in a kilometer-square detector and full sky coverage is achieved.

At lower energies the backgrounds are down-going cosmic ray muons, atmospheric neutrinos, and the dark noise signals produced by the photomultipliers themselves. The simulated trigger rate of down-going cosmic ray muons in IceCube is 1700 Hz while the rate of atmospheric neutrinos (ν_μ and $\bar{\nu}_\mu$) at trigger level is 300 per day. Depending on the type of signal to be searched for, this background is rejected using direction, energy, and neutrino flavor. At energies below 1 PeV, neutrino astronomy must focus on upward going neutrinos. At energies above 1 PeV, the cosmic ray muon background disappears while the low energy cosmic ray background can be rejected using an energy rejection cut. The background contribution from dark noise is not significant because the total dark noise rate of the optical sensor in situ is expected to be less than 0.5 kHz.

The highest sensitivity for astrophysical point sources can be achieved with muons. The muon channel stands out for two reasons: i) muons allow a sub-degree angular resolution over a wide energy range and ii) the effective volume for muons exceeds the geometric volume of the detector by factors of 10 to more than 50 depending on energy because of the muon range that is of order kilometers. Due to the long range of high energy muons the interaction of the ν_μ can be detected at distances of tens of kilometers outside the detector. We will here exclusively focus on the muon detection because it provides the benchmark sensitivity for some of the fundamental goals of high energy neutrino astronomy.

5.1. DETECTOR DESIGN

The detector consists of 4800 photomultipliers instrumenting a volume of 1 km^3 . The transmission of analogue PMT signals to the surface, used in AMANDA, has been abandoned. The photomultiplier signals will be captured and digitized inside the OM. The digitized signals are given a global time stamp with a precision of $<5 \text{ ns}$ and transmitted to the surface. The digital messages are sent to a string processor, a global event trigger and an event builder. All time calibrations will be automated. The geometry

of the detector will be measured to a precision of better than 2 m during deployment. It will be calibrated more precisely (< 1 m) with light flashers on-board the OM and also with cosmic ray muons. Both methods have been tested and successfully applied in AMANDA. High energy signals and complex events can be calibrated with powerful lasers deployed with the detector. Its absolute orientation can be determined from coincidences with the surface air shower array and by observation of the shadow of the moon, not possible with smaller detectors such as AMANDA. Once events are built in the surface DAQ, data will be processed and filtered. A reduced data set will be sent on a daily basis to the Northern hemisphere for further processing and data analysis. Twenty four hour satellite connectivity will be available for important messages. Construction of the detector is expected to commence in the Austral summer of 2004/2005 and continue for 6 years, possibly less. The growing detector will take data during construction, with each string coming online within days of deployment.

5.2. PERFORMANCE

5.2.1. Telescope Area

In detailed simulations based on AMANDA data, the response of the detector has been evaluated to cosmic ray muons, to atmospheric neutrinos and to a hypothetical E^{-2} cosmic neutrino spectrum generated by a generic shock acceleration mechanism [52]. The event rates, normalized to one year of on-time, are listed in Table 3. Listed are event rates at trigger level as well as for full event reconstruction, with cuts applied for the rejection of the cosmic ray muon background. This is referred to as “level 2”. The trigger consists of a minimum of 5 local coincidences; a local coincidence is between two adjacent PMT or a pair separated by at most one PMT. Background from misreconstructed down-going cosmic ray muons can be rejected by a straightforward cut in energy. For a cosmic neutrino flux of $E_\nu^2 \times dN_\nu/dE_\nu = 10^{-7} \text{ GeV (cm}^2 \text{ sr)}^{-1}$, roughly the final sensitivity of AMANDA-II[46], more than 1000 signal events per year are predicted. At this stage, the background of 10^5 events, consists mostly of atmospheric neutrinos[53] and prompt muons from charm decay in the atmosphere[54].

The usual way to characterize the performance of the detector is to evaluate the “effective detector area” which is defined as

$$A_{\text{eff}}(E_\mu, \Theta_\mu) = \frac{N_{\text{detected}}(E_\mu, \Theta_\mu)}{N_{\text{generated}}(E_\mu, \Theta_\mu)} \times A_{\text{gen}}. \quad (11)$$

$N_{\text{generated}}$ is the number of muons in the test sample with energy E_μ and incident zenith angle Θ_μ . The energy of the muon is defined at the point of closest approach to the center of the detector. N_{detected} is the number

TABLE 3. Event rates are given for 1 year of signal and background. The signal assumes a cosmic neutrino flux of $E_\nu^2 \times dN_\nu/dE_\nu = 10^{-7} \text{ s}^{-1} \text{ cm}^{-2} \text{ sr}^{-1} \text{ GeV}$, roughly the ultimate sensitivity of AMANDA-II. The calculation of atmospheric neutrino induced muon events is based on [53] and it includes the prompt component according to [54].

	Trigger	Level 2
Cosmic ν	3.3×10^3	1.1×10^3
Atm ν	8.2×10^5	9.6×10^4
Atm μ	4.1×10^{10}	10×10^4

of events that actually trigger the detector, or pass the cut level under consideration.

Figure 11 shows the effective area for four energy intervals as a function of the zenith angle of the incident muon track. The effective trigger area reaches one square kilometer at an energy of a few hundred GeV. Roughly 50% of all triggered events pass the “standard selection” (level 2), independent of the muon energy. The detector reaches an effective detection area of one square kilometer for upward moving muons in the TeV range. Importantly, above 100 TeV the selection allows the detection of down-going neutrinos for observation of the southern hemisphere ($\cos \theta > 0$). In the PeV range the effective area for down-going muons is above 0.6 km^2 , increasing towards the horizon. This means that IceCube can be operated as a full sky observatory for neutrinos with energy in excess of $\sim 1 \text{ PeV}$.

5.2.2. Angular Resolution

The angular resolution of the detector is relevant for the search for neutrinos from point sources. Exploiting the angular resolution of the detector, background events can be more easily eliminated by restricting the search to a small angular region around the known direction of the object under investigation. Using AMANDA techniques only, an angular resolution approaching 0.5° is achieved; see Fig.12. Significant improvement of this resolution is expected with the development of reconstruction algorithms that include amplitude and waveform information not provided by AMANDA detection methods.

5.2.3. Sensitivity to Astronomical Neutrino Fluxes

Diffuse Fluxes. As previously discussed, theoretical models of astrophysical fluxes of high energy neutrinos are often linked to the known flux of the

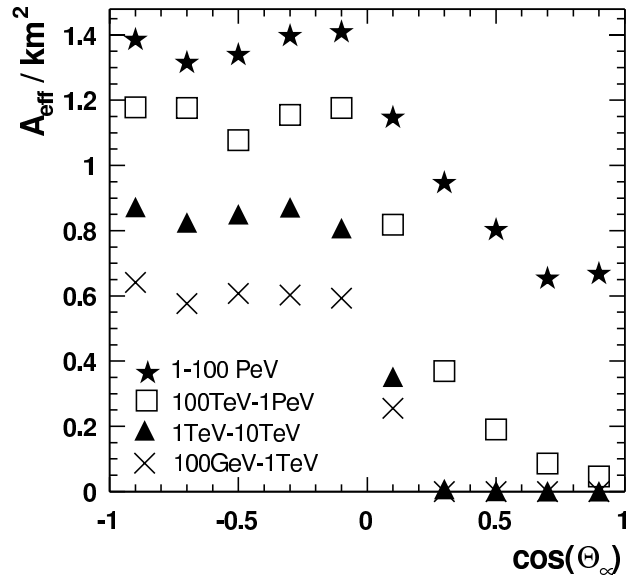


Figure 11. The effective area for neutrino-induced muons is shown as a function of the zenith angle after applying level 2 cuts.

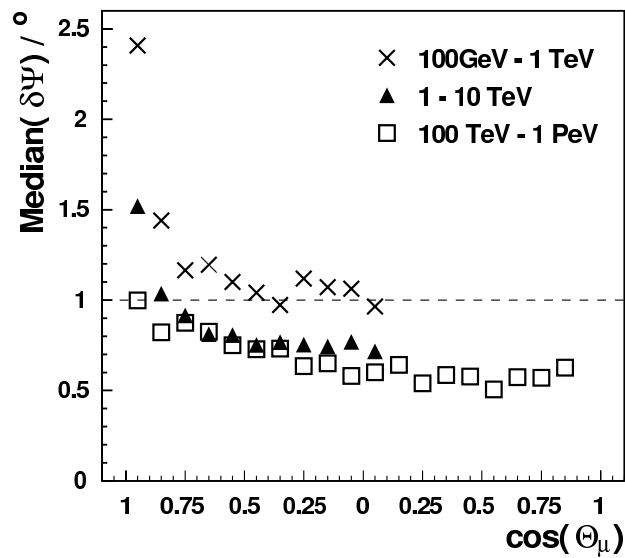


Figure 12. Pointing resolution for muons. Shown is the median space angle error of the reconstructed direction as a function of the zenith angle of the incident track.

very high energy cosmic rays of extragalactic origin; see Fig. 6. The harder energy spectrum, typically E^{-2} , expected for an astrophysical neutrino flux can be used to discriminate against the softer atmospheric neutrino background. The number of optical modules in an event that detect at least one photon, called the channel multiplicity N_{ch} , is used as a very simple and robust energy observable. Atmospheric neutrino-induced events have typical channel multiplicities of 30 to 60 channels. The assumed high energy signal dominates the atmospheric neutrino background above channel multiplicities in the vicinity of 200. For an optimized energy cut $N_{\text{ch}} > 227$, a simulated source with spectrum $E_\nu^2 \times dN_\nu/dE_\nu = 1 \times 10^{-7} \text{ GeV (cm}^2 \text{ s sr)}^{-1}$, previously introduced, results in 74 signal events in one year of operation compared to a background of 8 atmospheric neutrinos. The background was calculated including prompt decays of charmed mesons which may contribute as much as 80% to the final atmospheric sample following reference[54]. After three years of operation an overall flux limit of $E^2 \times dN_\nu/dE_\nu = 8.1 \times 10^{-9} \text{ GeV (cm}^2 \text{ s sr)}^{-1}$ is obtained. This is more than two orders of magnitude below the current limit obtained with AMANDA. The energy cut results in a detection threshold of 200 TeV. The sensitivity obtained after one year of data taking is well below the Waxman-Bahcall flux previously discussed.

Sensitivity to Point Sources. With greatly improved angular resolution, IceCube can search for point neutrino sources with a search window of one degree radius thus greatly reducing the background. The remaining small number of background atmospheric neutrinos in the search bin is rejected by a soft energy cut $N_{\text{ch}} > 30$. The cut eliminates atmospheric neutrinos of energies below 1 TeV allowing for an essentially background free detection. With these parameters an average flux upper limit of $E_\nu^2 \times dN_\nu/dE_\nu = 5.5 \times 10^{-9} \text{ s}^{-1} \text{ cm}^{-2} \text{ GeV}$ is obtained after one year of data taking. After five years of operation the sensitivity level will reach $E^2 \times dN_\nu/dE_\nu \sim 1.7 \times 10^{-9} \text{ s}^{-1} \text{ cm}^{-2} \text{ GeV}$.

Gamma Ray Burst Sensitivity. As discussed in the context of AMANDA, the short duration of gamma ray bursts allows for an essentially background-free search. The AMANDA analysis only covers GRB in the northern sky; with IceCube a full sky search is possible at high energy. For a rate of 500 bursts over $2\pi \text{ sr}$ and 1 year, 13 neutrino induced up-going muons are predicted on a background of 0.1. This rate corresponds to the standard fireball model normalized by the assumption that GRB are the sources of the highest energy cosmic rays.

5.2.4. Cascades and Very High Energy Neutrinos

Due to its large and uniformly instrumented volume, IceCube also has excellent sensitivity to cascades generated by ν_e , $\bar{\nu}_e$, ν_τ , and $\bar{\nu}_\tau$. At energies

above a few tens of TeV the detector becomes fully efficient to cascade detection with an effective volume comparable to the geometric volume of 1 km^3 ; see Fig. 13. At energies above 1 PeV tau events can be separated from ν_e -induced cascades using a variety of methods. For extremely energetic muons, effective areas well beyond the geometric area are achieved. Effective areas at 10^{18} eV are estimated to reach more than 2.5 km^2 . Reconstruction algorithms for the more complex event topologies such as from tau events and for extreme energies beyond 10^{18} eV are not fully developed yet. However, the high resolution and large dynamic range of the IceCube data acquisition system will provide rich information to extract the physics from such events.

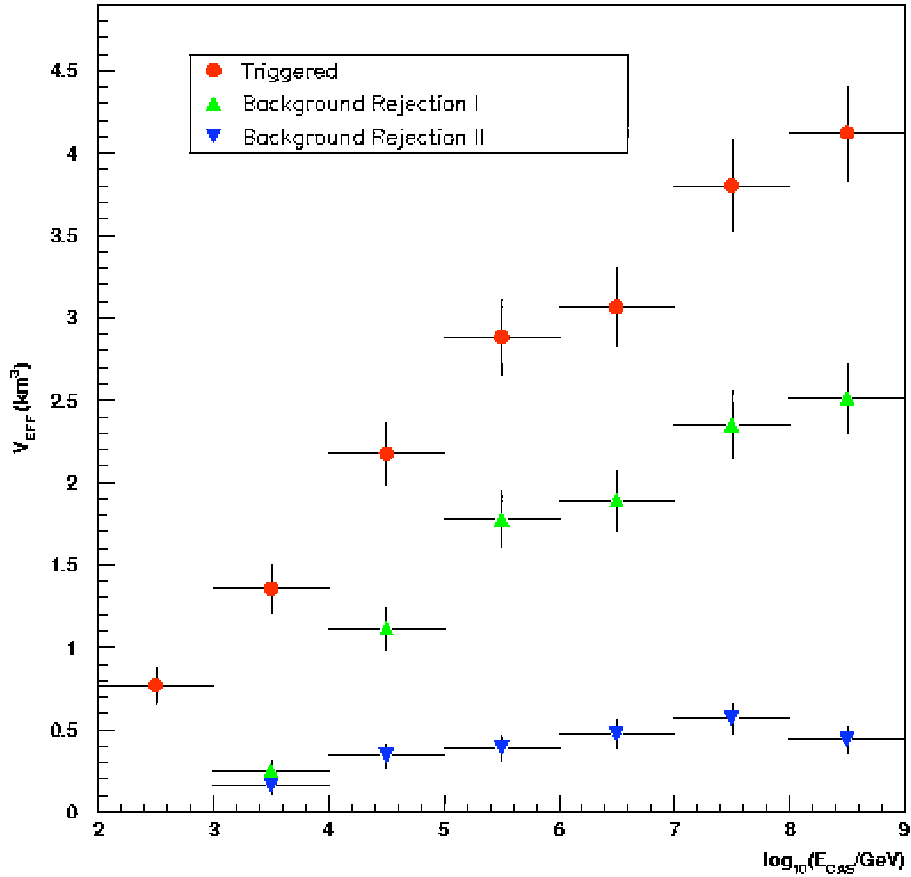


Figure 13. Effective volume for neutrino-induced cascades at trigger level (circles), after background suppression cuts (upward triangles), and both background cuts and requiring that the cascade falls within the volume of instrumented ice (downward triangles).

5.2.5. *Other Science Opportunities*

Dark Matter. If Weakly Interacting Massive Particles (WIMPs) are the dark matter of the Universe, they populate the galactic halo of our Galaxy. Some have been captured over astronomical times by the Earth and the sun where they annihilate pairwise, producing high-energy muon neutrinos that can be searched for by neutrino telescopes. A favorite WIMP candidate is the lightest neutralino of the Minimal Supersymmetric Model. The energy of the neutrino-induced muons is of order 25% of the neutralino mass. The predicted muon rates from WIMPs annihilating in the sun can be as large as 10^4 km^{-2} per year at 100 GeV and more than a 10^4 km^{-2} up to energies of 1 TeV. Current limits eliminate fluxes larger than several thousand events at energies above 100 GeV. Simulations indicate that IceCube should reach sensitivities below 50 muon events per year for WIMPs from the sun [55]. Thus IceCube will play a complementary role to future direct detection experiments like GENIUS for annihilation in the Earth, and be competitive with such next-generation direct detection experiments for annihilation in the Sun.

Cosmic Rays and Air Showers. Combined with the 1 km^2 surface detector, IceCube can do unique coincidence and anti-coincidence measurements of high energy air showers. In addition to providing a sample of events for calibration and for study of air-shower-induced backgrounds in IceCube, the surface array will also act as a partial veto. All events generated by showers with $E > 10^{15} \text{ eV}$ can be vetoed when the shower passes through the surface array. In addition, higher energy events, which are a potential source of background for neutrino-induced cascades, can be vetoed even for showers passing a long distance outside the array. The IceCube–IceTop coincidence data will cover an energy range starting below the knee of the cosmic-ray spectrum to $> 10^{18} \text{ eV}$. Each event will contain a measure of the shower size at the surface and a signal from the deep detector produced by muons with $E > 300 \text{ GeV}$ at production. At the high elevation of the South Pole, showers will be observed near shower maximum so that measured shower size provides a good measure of the total size and the energy. The combined measurement of the muon-induced signal in IceCube and the shower size at the surface will yield information on the primary composition over three orders of magnitude in energy. In particular, if the knee is due to a steepening of the rigidity spectrum, a steepening of the spectrum of protons around $3 \times 10^{15} \text{ eV}$ should be followed by a break in the spectrum of iron at $8 \times 10^{16} \text{ eV}$. The method for measuring composition has been developed and applied successfully with AMANDA and the surface air shower array SPASE-2 [56].

5.2.6. *Supernova Detection*

Although the MeV energies of supernova neutrinos are far below the AMANDA/IceCube trigger threshold, a supernova can be detected by observing higher counting rates of individual PMT over a time window of 5–10 seconds. The enhancement in rate of a single PMT will be buried in its dark noise. However, by summing the signals from all PMT over 10 s, significant excesses are observed. With background rates more than 10 times lower than ocean experiments, IceCube has the potential to see a supernova out to the LMC and to generate an alarm signal.

6. The Future Is Now

At this point in time, several new instruments such as HiRes, the partially deployed Auger array, Hess and Magic, Milagro, Baikal and AMANDA-II are taking data. With rapidly growing observational capabilities, one can express the realistic hope that the cosmic ray puzzle will be solved soon. The solution is likely to reveal unexpected astrophysics, if not particle physics.

Acknowledgments

This work was supported in part by DOE grant No. DE-FG02-95ER40896 and by the U.S. National Science Foundation, Office of Polar Programs; U.S. National Science Foundation, Physics Division and the University of Wisconsin Alumni Research Foundation.

References

1. D.J. Bird *et al.* (1993) *Phys. Rev. Lett.* **71**, 3401.
2. N.N. Efimov *et al.* (1991) *ICRR Symposium on Astrophysical Aspects of the Most Energetic Cosmic Rays*, ed. M. Nagano and F. Takahara, World Scientific.
3. http://www.hep.net/experiments/all_sites.html, provides information on experiments discussed in this review. For a few exceptions, we will give separate references to articles or websites.
4. M. Ave *et al.* (2000) *Phys. Rev. Lett.* **85**, 2244
5. <http://www.akeno.icrr.u-tokyo.ac.jp/AGASA/>
6. *Proceedings of the International Cosmic Ray Conference*, Hamburg, Germany, August 2001.
7. F.W. Stecker, M.H. Salamon (1992) *Astrophys. J.* **512**, 52, astro-ph/9808110
8. R.A. Vazquez *et al.* (1995) *Astroparticle Physics* **3**, 151.
9. J. Alvarez-Muniz, F. Halzen, T. Han, and D. Hooper, *Phys. Rev. Lett.* **88**, 021301, hep-ph/0107057; R. Emparan, M. Masip, and R. Rattazzi, *Phys. Rev. D* **65**, 064023, hep-ph/0109287; P. Jain, D.W. McKay, S. Panda, and J.P. Ralston, *Phys. Lett. B* **484**, 267, hep-ph/0001031; A. Jain, P. Jain, D.W. McKay, and J.P. Ralston, hep-ph/0011310; C. Tyler, A.V. Olinto, and G. Sigl, *Phys. Rev. D* **63**, 055001, hep-ph/0002257; S. Nussinov and R. Shrock, *Phys. Rev. D* **59**, 105002, hep-ph/9811323; S. Nussinov and R. Shrock, *Phys. Rev. D* **64**, 047702, hep-ph/0103043; G. Domokos and S. Kovesi-Domokos, *Phys. Rev. Lett.* **82**, 1366, hep-ph/9812260; G. Domokos, S. Kovesi-Domokos, and P.T. Mikulski, hep-ph/0006328.

10. E. C. Loh, these proceedings
11. F. W. Stecker, these proceedings
12. F. Halzen (1995) The case for a kilometer-scale neutrino detector, in *Nuclear and Particle Astrophysics and Cosmology*, Proceedings of Snowmass 94, ed. by R. Kolb, R. Peccei, World Scientific, Singapore; F. Halzen (1996) The case for a kilometer-scale neutrino detector: 1996, *Proc. of the Sixth International Symposium on Neutrino Telescopes*, ed. by M. Baldo-Ceolin, Univ. of Padua.
13. J.N. Bahcall and E. Waxman (2001) *Phys. Rev. D* **64**, 023002, hep-ph/9902383.
14. E. Waxman and J.N. Bahcall (1999) *Phys. Rev. D* **59** 023002, hep-ph/9807282.
15. K. Mannheim, R.J. Protheroe, and J.P. Rachen (2001) *Phys. Rev. D* **63**, 023003, astro-ph/9812398
16. J.P. Rachen, R.J. Protheroe, and K. Mannheim (1998), talk presented at *The 19th Texas Symposium on Relativistic Astrophysics: Texas in Paris*, Paris, France, 14–18 Dec, 1998, astro-ph/9908031.
17. F. Halzen and E. Zas (1997) *Astrophys. J.* **488**, 669, astro-ph/9702193
18. J. Alvarez-Muniz and F. Halzen, *Astrophys.J.*576:L33-L36, astro-ph/0205408].
19. T.K. Gaisser, R.J. Protheroe, and T. Stanev (1998) *Ap.J.* **492**, 219.
20. L. O’C. Drury, F.A. Aharonian, and H.J. Völk (1994) *A & A* **287**, 959.
21. J.A. Esposito, S.D. Hunter, G. Kanbach, and P. Sreekumar (1996) *Ap.J.* **461**, 820.
22. W. Bednarek and R. J. Protheroe (1997) *Phys. Rev. Lett.* **79**, 2616.
23. The Cangaroo collaboration (2002) *Nature* **416**, 797.
24. C. Barbot, M. Drees, F. Halzen, and D. W. Hooper (2002) report nos. TUM-HEP-463-02, MADPH-01-1270, hep-ph/0205230.
25. T. K. Gaisser, F. Halzen, and T. Stanev (1995) *Phys. Rept.* **258**, 173 [Erratum **271**, 355 (1995)], hep-ph/9410384; J.G. Learned and K. Mannheim (2000) *Ann. Rev. Nucl. Part. Science* **50**, 679.
26. K. Greisen (1960) *Ann. Rev. Nucl. Science* **10**, 63.
27. F. Reines (1960) *Ann. Rev. Nucl. Science* **10**, 1.
28. M.A. Markov and I.M. Zheleznykh (1961) *Nucl. Phys.* **27**, 385.
29. M. A. Markov (1960) in *Proceedings of the 1960 Annual International Conference on High-energy Physics at Rochester*, ed. by E.C.G. Sudarshan, J.H. Tinlot, and A.C. Melissinos.
30. J. Babson *et al.*, for the DUMAND Collaboration (1990) Cosmic Rays in the Deep Ocean, ICR-205-89-22, Dec. 1989, 24 pp., *Phys. Rev. D* **42**, 3613.
31. I.A. Belolaptikov *et al.* (1997) *Astroparticle Physics* **7**, 263.
32. V.A. Balkanov *et al.* (2000) *Astro. Part. Phys.* **14**, 61.
33. E. Aslanides *et al.* (1999), astro-ph/9907432.
34. F. Feinstein, for the ANTARES Collaboration (1999) *Nucl. Phys. Proc. Suppl.* **70**, 445.
35. T. Montaruli, for the ANTARES Collaboration (2001) *Proceedings of TAUP 2001: Topics in Astroparticle and Underground Physics*, Assergi, Italy, 8–12 Sept. 2001, hep-ex/0201009.
36. L. Trasatti (1999) *Procs. of the 5th International Workshop on Topics in Astroparticle and Underground Physics (TAUP 97)*, Gran Sasso, Italy, 1997, ed. by A. Bottino, A. di Credico, and P. Monacelli *Nucl. Phys. B Proc. Suppl.* **70**, 442.
37. P.K. Grieder, for the NESTOR Collaboration (2001) *Nuovo Cim.* **24C**, 771.
38. Talk given at the *International Workshop on Next Generation Nucleon Decay and Neutrino Detector (NNN 99)*, Stony Brook, 1999, Proceedings ed. by M.V. Diwan and C.K. Jung (AIP Conf. Proc., NY) vol. **533** (2000).
39. P.B. Price, K. Woschnagg, and D. Chirkin (2000) *Geophys. Res. Lett.* **27** 2129.
40. E. Andres *et al.* (2001) *Nature* **410**, 441–443.
41. J. Ahrens *et al.* (2000) *Phys. Rev. D* **66**, 012005.
42. J. Ahrens *et al.* (2000) *Phys. Rev. D* **66**, 032006.
43. P. Niessen and C. Spiering for the AMANDA collaboration, in *Proc. of ICRC*, Hamburg, Germany, 2001, p. 1496.

44. S. Hundertmark for the AMANDA Collaboration, contributed poster I-1, this conference; S. Hundertmark for the AMANDA Collaboration, in *Proc. of the Second Workshop on Methodical Aspects of Underwater/Underice Neutrino Telescopes*, Hamburg, 2001.
45. J. Ahrens *et al.* (2002) submitted to *Astrophysical Journal*.
46. G.C. Hill and M.J. Leuthold for the AMANDA Collaboration (2001), in *Proc. of ICRC*, Hamburg, Germany, 2001, p. 1113, and submitted to *Phys. Rev. Letters* (2002).
47. J. Ahrens *et al.* (2001) *Astropart. Phys.* **16**, 345–359.
48. M. Kowalski and I. Taboada for the AMANDA Collaboration, in *Proc. of the Second Workshop on Methodical Aspects of Underwater/Ice Neutrino Telescopes*, Hamburg, Germany, 2001; M. Kowalski (2002) Ph.D. Thesis, Humboldt University, Berlin; I. Taboada (2002) Ph.D. Thesis, University of Pennsylvania, Philadelphia, USA.
49. J. Ahrens *et al.*, submitted to *Phys. Rev. D* (2002).
50. E. Waxman and J. N. Bahcall (1997) *Phys. Rev. Lett.* **78**, 2292-2295; for a detailed calculation of event rates, see J. Alvarez-Muniz, F. Halzen and D. W. Hooper (2000) *Phys. Rev. D* **62** 093015.
51. R. Hardtke (2002) Ph.D. Thesis, UW-Madison and to be published.
52. See Preliminary Design Document at <http://icecube.wisc.edu/science/sci-tech-docs/> and J. Ahrens *et al.* (2002) Sensitivity of the IceCube Detector to Astrophysical Sources of High Energy Muon Neutrinos, to be published.
53. P. Lipari (1993) *Astropart. Phys* **1** 195-227.
54. E.V. Bugaev *et al.* (1998) *Phys. Rev. D* **58**, 054001.
55. J. Edsjo (2000) WIMP searches with IceCube, Amanda Internal report.
56. K. Rawlins (2001) Ph.D. Thesis, UW-Madison and <http://amanda.physics.wisc.edu/Docs/>